A Study of Microstructure and Mechanical Properties of Metal Injection Moulded HK-30

Martin A. Kearns, Toby A. Tingskog, Andrew J. Coleman, Keith Murray,
Viacheslav Ryabinin* and Erainy Gonzalez *

Sandvik Osprey Ltd., Red Jacket Works, Milland Road, Neath, SA11 1NJ, United Kingdom
* TCK S.A., Zona Franca Industrial Las Americas, Santo Domingo, Dominican Republic

ABSTRACT

Metal Injection Moulding has been adopted for the manufacture of a variety of high temperature turbocharger components in recent years, successfully displacing precision casting or machining processes. The operating environment demands very good high temperature wear and corrosion resistance coupled with excellent fatigue properties. Highly alloyed stainless steels such as AISI 310 and HK-30 (UNSJ94203) are therefore commonly used for manufacture of turbocharger vanes. Control of carbon level and distribution in the finished components is critical to control final grain size and properties and it is essential that the relationship between powder characteristics, including chemistry, and MIM processing parameters are well understood so that these requirements can be achieved. In this study we explore the effect of particle size distribution and chemistry on MIM component densities and metallurgical properties with a particular focus on grain size and density. The effect of sintering temperature and atmosphere are also evaluated and room temperature mechanical properties presented.

INTRODUCTION

The adoption of turbocharger technology in automotive engines has been responsible for significant improvements in engine efficiency and fuel economy. In particular, VGT (variable geometry turbo) or VNT (variable nozzle turbo)[(1)] designs enable control of exhaust air flow to maintain optimum performance at low and high engine speeds via adjustment of turbine vane geometry. An example of vane geometry is shown in Fig. 1 below.

Fig. 1 Example of MIM'ed turbocharger vane.

The service environment for turbo vanes is demanding, with erosion and corrosion attack from high temperature exhaust gases. As well as excellent hot-wear and corrosion resistance, the chosen alloy must have good high temperature fatigue and creep strength and microstructural stability at operating temperatures which, for diesel engines, can reach ~850^{o}C. Heat resistant stainless steels offer a good combination of hot strength, corrosion resistance and creep / fatigue life [(2)]. A modified 310 stainless steel grade known as HK-30 is a popular choice, featuring Nb addition to give a fine dispersion of stable carbides for strengthening purposes and Si addition to increase resistance to carburisation. On prolonged exposure to high temperature, such alloys can be susceptible to long term embrittlement due to formation of sigma phase [(3)] and, for this reason, Si is limited to ~2% max. Control of carbon level is important in order to achieve desired strength levels and a fine grain size is desirable for optimum strength and toughness. High Cr and Ni confer excellent resistance to hot corrosion, including sulphur-bearing atmospheres, under both oxidizing and reducing conditions.

HK-30 is usually used in the as-cast condition, e.g. for furnace tubes, calcining plant and hydrocarbon pyrolysis tubing. Its starting microstructure consists of an austenite matrix with fine dispersions of carbides (Cr rich $M_{23}C_6$ or Nb-rich MC). During service, precipitation of sigma-phase occurs in the range 620 to 900°C and has a deleterious effect on mechanical properties. Formation of sigma phase in HK-30 can occur directly from austenite in the range 760 to 870°C particularly at lower carbon levels (0.20-0.30%) and this can lead to significant scatter in properties at intermediate temperatures.
MIM can offer advantages over a cast route in providing near net shape, good surface finish and refined, homogeneous microstructures compared with investment cast parts.
Table 1 shows published data for as sintered and heat treated MIM and wrought AISI 310 alloys.

Table 1: Published values for HK-30

Form	UTS MPa (ksi)	0.2%PS MPa (ksi)	El %	Density g/cm^3	Density %TD	Hv 5/25	Hardness HRB	Grain size µm (ASTM#)
MIM N_2, 1300°C[4]	730 (106)	332 (48)	12.5	7.65	97.9	247	90	60-70 (5)
MIM Ar, 1300°C[4]	560 (81)	194 (28)	33.4	7.50	96.6	162	78	30-40 (6-7)
IMET 310N [5]	650 (94)	380 (55)	7	>7.55	>97.4	220	-	-
Wrought 310	655 (95)	310 (45)	45	7.75	100	-	85	-

In this study we evaluate the sintered properties of HK-30 made using prealloyed powders at two popular size distributions. Two sintering temperatures were chosen guided by Thermocalc modelling of phase stability. Recognising the criticality of carbon control, one objective of the current study is to evaluate benefits of low-oxygen gas atomised powders on control of chemistry and therefore finished parts properties. A further goal was to seek to control grain size through controlled minor alloying additions.

EXPERIMENTAL PROCEDURE

A series of prealloyed HK-30 based powders was produced by Sandvik Osprey's proprietary inert gas atomisation process using nitrogen gas. The 'as-atomised' powders were air classified to either of two typical particle size distributions: 90%-22µm or 80%-22µm. The chemistry of each powder batch used in the study is shown in Table 2. Note that the 'A' suffix is the normal HK-30 specification while the alloys with suffix B and C represent alloys doped with increasing additions of additives to control grain size.

Table 2: Chemical analysis of powders used in this study.

Alloy	Fe	Cr	Ni	Nb	Mn	Si	Mo	N	C	P	S	O
HK-30A	Bal	25.4	19.8	1.31	1.19	1.29	0.16		0.30	0.025	0.004	
HK-30B	Bal	24.9	19.9	1.33	1.21	1.44	0.08	0.15	0.32	0.019	0.004	0.066
HK-30C	Bal	25.3	20.0	1.32	1.16	1.47	0.16	0.16	0.33	0.020	0.004	0.077

The particle size distributions of the powders used in this study are shown in Table 3 along with tap density values and the Melt Flow Index for each feedstock. This suggests that in general, as expected, feedstock made with coarser prealloy powder has lower viscosity than that made with finer powder.
Feedstocks were prepared by TCK using their proprietary binder formulation and aiming for a 16.0% shrinkage factor, typical of previous studies with prealloyed gas atomised powders. The shrinkage factor is the scale factor applied to the target final part dimensions in order to design the mould. The feedstocks were moulded in an Arburg injection moulding unit and sintered by TCK in an Elnik furnace, to produce standard MIMA tensile and Charpy test specimens.

Table 3: Particle size & Melt Flow Index (MFI) data

Alloy	Particle Size (µm)	MFR, g/min	Tap Density gcm^{-3}	Particle Size Data (µm)		
				D90	D50	D10
HK-30A	90%-22µm	177.2	4.83	21.5	9.7	3.6
HK-30B	90%-22µm	200.3	4.76	21.6	12.8	4.2
HK30C	90%-22µm	152.0	4.47	21.9	11.5	4.7
HK-30A	80%-22µm	222.2	4.76	27.9	11.3	3.7
HK-30B	80%-22µm	214.1	4.93	28.5	13.3	4.6
HK-30C	80%-22µm	144.6	4.87	26.7	13.6	5.2

Moulded green parts were subject to an initial solvent debind followed by thermal debind at 500°C (932°F) for 3.5h and sintered in a nitrogen atmosphere. Two sintering cycles were run at 1280°C and 1300°C:

- Run 1: 2°C /min ramp to 1000°C, 60 min hold, 2°C/min ramp to 1280°C, 60 min hold, furnace cool.
- Run 2: 2°C /min ramp to 1000°C, 60 min hold, 2°C/min ramp to 1300°C, 60 min hold, furnace cool.

Charpy bars were suspended both cantilever style (20mm overhang) and across refractory supports, (38mm separation) to determine the extent of distortion as a function of chemistry, particle size range and sintering temperature. Sintered parts were allowed to slow cool under a nitrogen atmosphere. As-sintered tensile samples were tested in triplicate in accordance with ASTM E8-08. Vickers hardness testing was carried out on tensile bar tabs using a 10kg weight. Sintered density measurements were carried out using a Micromeritics Accupyc II1340 Helium Pycnometer. Polished cross-sections of Charpy bars were prepared for microstructural analysis by etching in dilute aqua regia.

RESULTS

As-sintered parts were analysed to determine tensile properties, hardness and %C content. Table 4 shows the test values. The results show that carbon content was well controlled in all cases with a predictable loss of 0.02-0.03% from the level in the starting powder.

Table 4: Properties of as-sintered bars.

Alloy	Particle Size, µm	Sinter Temp, °C	UTS, MPa	0.2%PS, MPa	%El	Density, g/cm^3	Density, %TD	Hardness VHN	%C	Change in %C
HK-30A	90%-22	1280	822	456	11.0	7.41	95.21	237	0.27	-0.03
		1300				7.74	99.46		0.27	
	80%-22	1280	830	459	11.5	7.38	94.74	225	0.27	
		1300				7.72	99.10		0.27	
HK-30B	90%-22	1280	590	371	2.0	7.55	97.41	181	0.28	-0.03
		1300				7.72	99.66		0.30	
	80%-22	1280	527	335	2.3	7.64	97.90	155	0.29	
		1300				7.71	98.77		0.30	
HK30C	90%-22	1280	756	441	8.3	7.22	92.52	211	0.31	-0.02
		1300				7.70	98.74		0.32	
	80%-22	1280	605	369	2.0	7.50	96.63	196	0.30	
		1300				7.67	98.85		0.33	

Results show that raising the sintering temperature from 1280 to 1300°C has a very significant effect on sintered density with all alloy variants and particle sizes achieving near to full density at 1300°C. At

1280°C, there is a spread in parts density with variant B showing highest density. The effect of particle size distribution on final density is variable with finer particle size distribution being generally marginally beneficial with the exception of variant C at 1280°C.

Fig. 2 Sintered density vs alloy, particle size and sintering temperature. Theoretical density is 7.75g/cm^3.

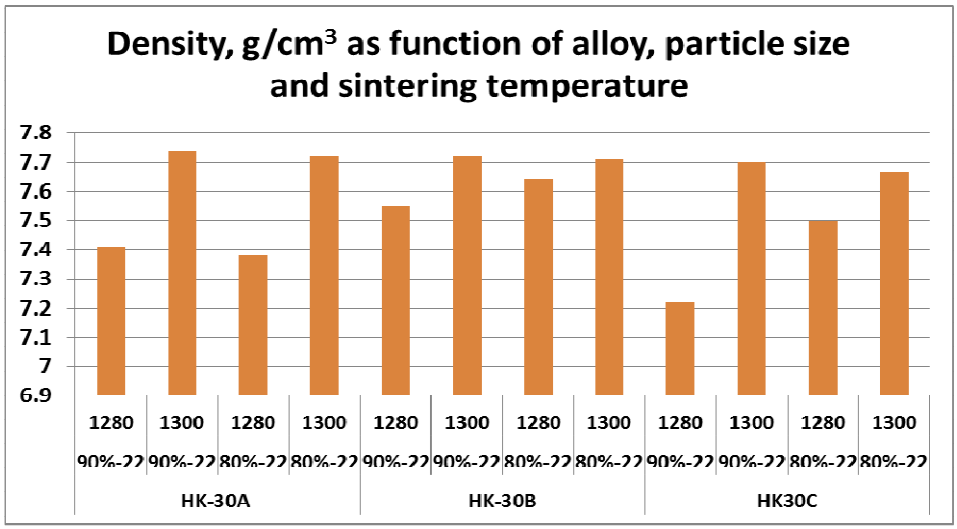

Table 5 shows the effect of different variables on the distortions measured on cantilevered and suspended specimens. Here it is apparent that distortions are greater at the higher sintering temperature and that finer powder size distribution is beneficial in reducing distortion. It may also be noted that increasing the level of grain refining additive leads to lower distortion.

Table 5: Effect of particle size and sintering temperature on Charpy bar deflections

Alloy	Particle Size, µm	Sinter Temp,°C	Cantilever deflection, mm	Suspended deflection, mm
HK-30A	90%-22	1280	1.750	1.33
		1300	1.478	1.344
	80%-22	1280	2.118	1.25
		1300	broken	1.173
HK-30B	90%-22	1280	broken	1.325
		1300	2.842	1.123
	80%-22	1280	broken	1.569
		1300	2.156	1.324
HK-30C	90%-22	1280	2.727	0.896
		1300	1.027	0.994
	80%-22	1280	2.936	0.882
		1300	1.499	1.569

Metallographic analysis was carried out on samples from each sintering run and powder type. Images of the polished microstructures for selected variants at 1280°C and 1300°C sintering temperatures are shown in Figures 4 and 5. The porosity seen in HK-30A sintered at 1280°C is much less than in HK-30B. HK-30C, with largest grain refiner addition has larger pores than 'A' but less frequent than 'B'. In samples 'A' and 'C', the grains show pronounced intragranular precipitations of NbC and the grain structure appears more refined in sample 'C' compared with 'A' and the NbC precipitates are smaller and more frequent in 'C'. A lamellar structure can also be detected within some grains in sample 'A' but not in 'C'.

The lamellar structure is more common at the sample surface suggesting it is a nitride of some type. Overall, carbides appear to be distributed evenly in all samples with carbide size reflecting the grain size.

Fig. 3 Deflection of Charpy bars as a function of alloy variant, particle size and sintering temperature.

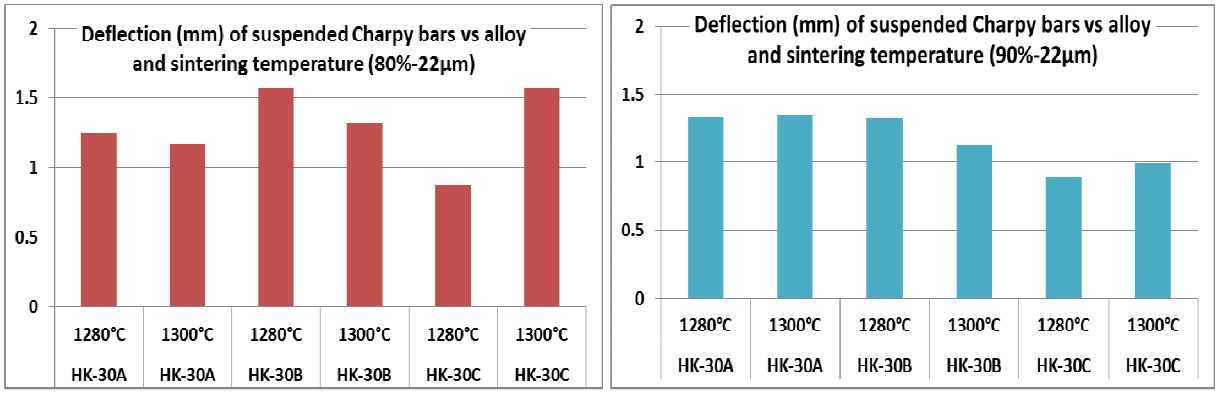

Figure 4: Micrographs of polished samples from the two sintering cycles: a) 1280°C and b) 1300°C

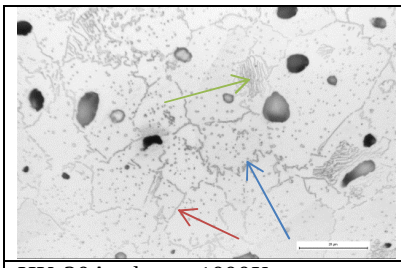	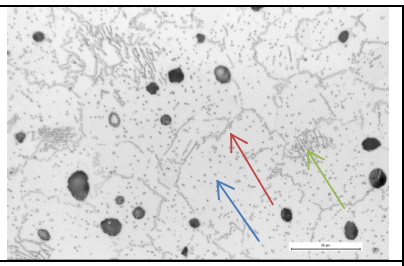	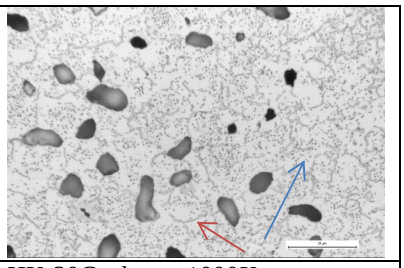
HK-30A, charpy 1000X Carbide = blue Grain boundary precipitate = red Lamellar structure = green	HK-30A, charpy 1000X Carbide = blue Grain boundary precipitate = red Lamellar structure = green	HK-30C, charpy 1000X Carbide = blue Grain boundary precipitate = red Lamellar structure = green

The ASTM-grain size was evaluated from micrographs and results can be seen in Table 6 Not all samples could be easily evaluated for ASTM number. At first glance sample 'B' seem to be over-etched but at higher magnifications it can be seen that the samples contain a lot of precipitates. Because of the large number of precipitates it is very difficult to decide a grain size.

Sample	HK-30A 80%-22	HK-30A 90%-22	HK-30B 80%-22	HK-30B 90%-22	HK-30C 80%-22	HK-30C 90%-22
ASTM	7-8	7-8	tbd	tbd	trd	11
Comment	more even than 90%-22	also smaller grains	not possible to decide because of precipitations	not possible to decide because of precipitations	not possible to decide because of precipitations	very fine grain size

Mechanical Properties

The tensile properties reported in Table 4 for parts sintered at 1280°C show good tensile strength and ductility in regular HK-30 despite their relatively low density. The increasing addition of grain refiner appears at first ('B') to have caused a significant reduction in strength and ductility, despite an increase in density. However a further increase in grain refiner addition ('C') gives a strength value which

approaches regular HK-30 but again with lower density. This trend is depicted in Fig 5. Worst results are comparable with cast values, while other values compare well with results published elsewhere [4, 5].

Fig. 5: Mechanical properties of HK30 variants sintered at 1280°C

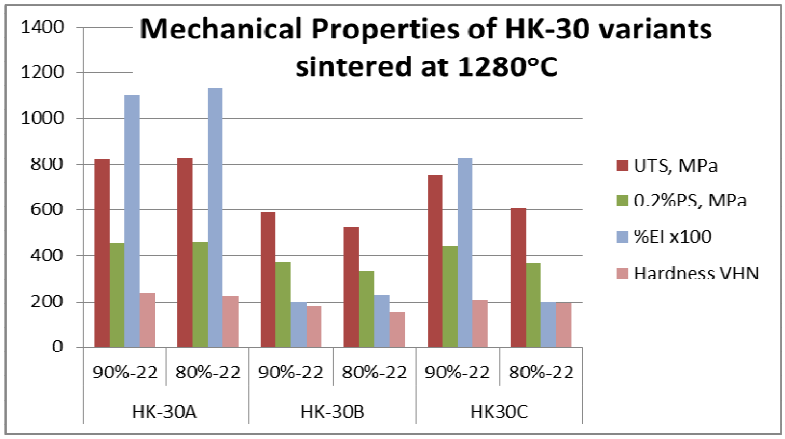

Fig 6: Mechanical properties of HK-30 variants sintered at 1300°C

Sintering at 1300°C produces a much higher finished part density and metallography shows that in all cases, there has been a degree of grain coarsening and carbide coarsening. The increased density drives towards higher strength and ductility, but the coarsening effect moderates the observed increases. It may be noted that hardness values tend to mirror changes in proof strength as expected (Table 4).

DISCUSSION

The sintering cycles chosen for these studies were influenced by Thermocalc studies that indicated that liquid phase should begin to become evident at ~1280°C and that the volume fraction of liquid phase would rise sharply beyond that point – see Figure 7. The equilibrium was also calculated at 1280ºC and shows that two phases are expected to be stable at this temperature: austenite and NbC (fcc phase containing ~84wt% Nb and 11% C). The latter fits well with separate EDS analysis of the precipitates. At this sintering temperature calculations shows no presence of liquid phase. However liquid phase is predicted at temperatures just above 1280°C. The increase in densification apparent when going from 1280 to 1300°C is therefore understandable and this highlights the sensitivity of the alloy to a narrow sintering window. If the temperature is too low, densification will be incomplete and shrinkage more erratic, while if the temperature is excessive, slumping of the parts is expected to be more likely to occur. Certainly this study bears out the fact that at 1300°C, virtually full densification occurs with a ~3-4% enhancement in theoretical density vs 1280°C sintering. However, slump tests do not suggest a major influence of sintering temperature on deflection of parts, though on average, the finer size distribution (90%-22µm) shows a slightly lower deflection and the higher addition of grain refiner in the 90%-22µm variant gives lowest deflection of all.

The narrow sintering window referred to above requires that carbon level in particular is well controlled. If not, variable densification is expected. Data in Table 4 demonstrates that there is a small and consistent carbon loss on sintering for all the different alloys and conditions evaluated. This is to be expected in view of the low and consistent oxygen level found in the starting powder. Indeed the measured oxygen level of ~0.07% would equate to a loss in carbon of ~0.03% if converted to and lost as CO_2. The microstructure of the sintered parts shows varying amounts of residual porosity particularly in parts sintered at 1280°C and this is in part responsible for the variable ductility seen in these specimens which in turn leads to low UTS values. The role of the grain refiner additions on the microstructure has yet to be detailed, but it is surprising that the intermediate 'B' specimens display relatively high density but low strength levels. The effective grain refinement seen with the higher addition in 'C' samples appears to lead to enhanced strength levels though it is not clear whether this is responsible for the low deflection in these samples. Samples sintered at

Fig. 7: Thermocalc analysis of the HK-30 system

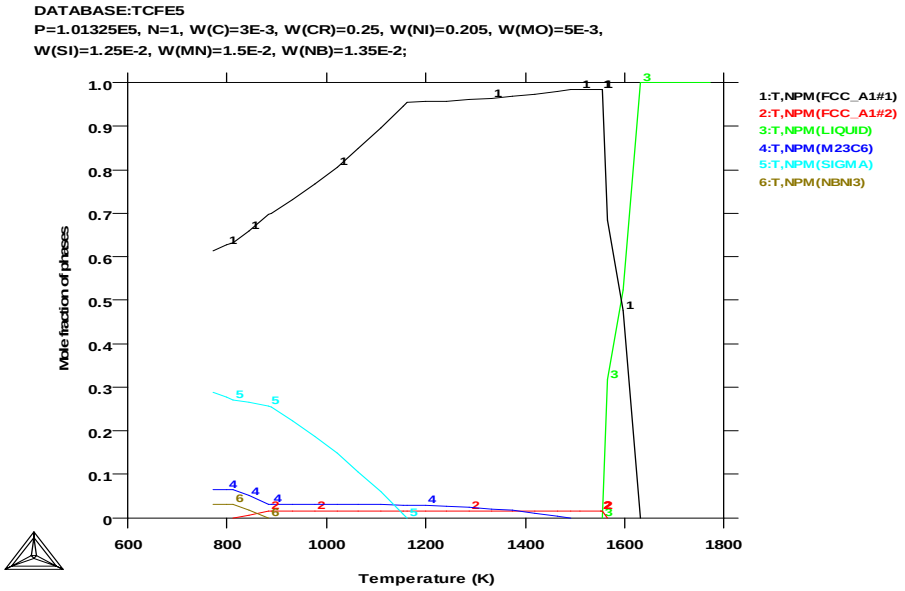

1300°C…….. Certainly it appears that the uniform distribution of fine NbC within the grains of all samples is particularly refined in the 'C' samples. The observation of grain boundary phases and lamellar phases is consistent with previous studies of these alloys and the predominance of the lamellar phase at surfaces suggests that the eutectoid is rich in nitrogen. Ref x mentions a 'lamellar phase resembling pearlite is often observed in HK alloys which is believed to be an austenite, carbonitride eutectoid and, except when present in excessive amounts, it is not associated with loss of hot strength. Untransformed ferrite is undesirable since this will transform to the brittle sigma phase if the alloy is held for more than short times around 816°C.

The addition of grain refiner elements leads to a change in the distribution of porosity at 1280°C, but at 1300°C, all specimens achieve high density. The refined products show an ASTM grain size of xxxx which compares with xxxx. This is reflected to some extent in the mechanical property measurements shown in Table xx.

The mechanical test data may be compared with those reported recently by Wang et al who examined the effects of sintering HK-30 in nitrogen and argon atmospheres at 1300°C. Their results, shown in Table 1 demonstrate that sintering in nitrogen enhances strength levels and this would be expected wither as a solid solution strengthening agent or, more likely, combined with nitride formers in the lamellar eutectoid phase. The strength levels reported for samples sintered in argon are very modest, though here the ductility values are correspondingly high, despite their lower density. The other striking feature they report is the fine grain structure obtained in Ar relative to nitrogen. The reason for this may be associated with a lack of grain boundary diffusion promoted by nitrogen/nitride formation but this would need to be confirmed.

SUMMARY AND CONCLUSIONS

The present study shows that sintering in nitrogen at 1300°C is effective in achieving virtually full density with either 90%-22µm or 80%-22µm HK-30 powders. The densification behavior in the range 1280-1300°C is accurately predicted by Thermocalc analysis. Room temperature tensile properties obtained by MIM are excellent and exceed other literature values. Control of carbon is excellent: there is a good correlation between levels in the starting powders and finished products. The microstructures reveal a uniform distribution of fine intragranular NbC and there is evidence of the lamellar eutectoid phase …

The addition of small amounts of grain refining agents to the powder prealloy are effective in achieving grain refinement without sacrificing densification or mechanical properties at 1300°C sintering temperature. The

additions are also effective in reducing some of the distortions that occur at high temperature. This behavior contrasts with the behavior reported in other studies where grain refinement achieved by sintering in Argon gas resulted in much inferior mechanical properties. It is therefore concluded that gas atomized HK-30 powders are ideally suited to producing high performance turbocharger components to close tolerances with excellent control of carbon leading to uniform shrinkage and predictable properties. By proprietary modification of the base alloy, it is also possible to achieve significant grain refinement and this may be desirable for certain service conditions.

ACKNOWLEDGEMENTS

Thanks are due to Ms Linn Larsson of Sandvik Materials Technology for Thermocalc studies and metallographic analyses; also to Mr Chris Phillips of Sandvik Osprey for deflection measurements. We are grateful also to Swansea University Dept of Materials Engineering for provision of Thermal Analysis data as part of the MACH 1 initiative.

REFERENCES

1. e.g. http://www.turbos.bwauto.com/products/vtg.aspx
   http://turbo.honeywell.com/our-technologies/vnt-turbochargers/
2. J.R.Davis, 'Stainless Steels', ASM International, Metals Park, Ohio, 1994.
3. A. M. Babakr, A. Al-Ahmari, K. Al-Jumayiah, F. Habiby, 'Sigma Phase Formation and Embrittlement of Cast Iron-Chromium-Nickel (Fe-Cr-Ni) Alloys'. Journal of Minerals & Materials Characterization & Engineering, Vol. 7, No.2, pp 127-145, 2008.
4. W.Wang, M.Ouyang, D Ye, J. Song, F. Pen,& Y. Yu (Xiamen Honglu Ltd) Z.Zhuang . Proc. Conf. APMA 2013 Xiamen, China, 3-6 Nov 2013. Reported in PIM International March 2014 Vol 8(1)
5. http://www.gkn.com/sintermetals/capabilities/MIM/Documents/MIM%20Materials.pdf
6. M.Bulger et al, MIM2010 Conference, MIM Component Distortion as a Function of Solids Loading